An Investigation of the Hydrogen-Bonding Structure in Bilirubin by ^{1}H Double-Quantum Magic-Angle Spinning Solid-State NMR Spectroscopy

Steven P. Brown,[†,§] Xiao Xia Zhu,[‡] Kay Saalwächter,[†] and Hans Wolfgang Spiess*[,†]

Max-Planck-Institut für Polymerforschung, Postfach 3148, D-55021 Mainz, Germany, and Département de Chimie, Université de Montréal, C.P. 6128 succursale Centre-ville, Montréal, Quebec H3C 3J7, Canada

Received December 11, 2000. Revised Manuscript Received February 20, 2001

Abstract: The complex hydrogen-bonding arrangement in the biologically important molecule bilirubin IXα is probed by using ^{1}H double-quantum (DQ) magic-angle spinning (MAS) NMR spectroscopy. Employing fast MAS (30 kHz) and a high magnetic field (16.4 T), three low-field resonances corresponding to the different hydrogen-bonding protons are resolved in a ^{1}H MAS NMR spectrum of bilirubin. These resonances are assigned on the basis of the proton−proton proximities identified from a two-dimensional rotor-synchronized ^{1}H DQ MAS NMR spectrum. An analysis of ^{1}H DQ MAS spinning-sideband patterns for the NH protons in bilirubin allows the quantitative determination of proton−proton distances and the geometry. The validity of this procedure is proven by simulated spectra for a model three-spin system, which show that the shortest distance can be determined to a very high degree of accuracy. The distance between the lactam and pyrrole NH protons in bilirubin is determined to be 0.186 ± 0.002 nm (corresponding to a dominant dipolar coupling constant of 18.5 ± 0.5 kHz). The analysis also yields a distance between the lactam NH and carboxylic acid OH protons of 0.230 ± 0.008 nm (corresponding to a perturbing dipolar coupling constant of 9.9 ± 1.0 kHz) and an H−H−H angle of 122 ± 4°. Finally, a comparison of ^{1}H DQ MAS spinning-sideband patterns for bilirubin and its dimethyl ester reveals a significantly longer distance between the two NH protons in the latter case.

Introduction

Structure determination by single-crystal X-ray diffraction methods is usually not sufficient for the localization of lighter atoms. This is of particular relevance with regard to the localization of hydrogen-bonded protons in biological structures, in which case a neutron diffraction study on deuterated samples is preferred.[1] Because of the dependence of the dipolar coupling between two nuclei on the internuclear separation to the inverse cubed power, solid-state NMR can be used to determine specific distance constraints. This information is particularly helpful if X-ray structures of the same or related compounds are available. Specifically, the rotational-echo double-resonance (REDOR)[2] technique is routinely used to study, in particular, biological systems.[3] Moreover, elaborate methods even allow the determination of torsional angles.[4] A significant restriction of all these methods, however, is the requirement to introduce isotopic labels, usually ^{13}C or ^{15}N, such that only particular dipolar-coupled spin pairs are present.

One of the most important recent advances in solid-state NMR has been the development of magic-angle spinning (MAS) probes capable of supporting ever greater rotation frequencies, ν_R.[5] A particularly promising application for this new technology is ^{1}H solid-state NMR, where, until recently, as described by Dec et al.,[6] the resolution achieved by a MAS-only approach was significantly inferior to that achievable by the technically very demanding combined rotation and multiple-pulse spectroscopy (CRAMPS)[7] method. Taking advantage of the enhanced line narrowing afforded by a ν_R above 25 kHz, it has been shown that the resulting resolution in ^{1}H MAS NMR spectra of typical organic solids is sufficient to allow ^{1}H resonances due to chemically distinct protons to be distinguished.[8−10]

By the combination of fast MAS with two-dimensional double-quantum (DQ) spectroscopy,[11,12] the structural and dynamic information inherent to proton−proton dipolar couplings can be probed. Specifically, we have recently demon-

* To whom correspondence should be addressed.
† Max-Planck-Institut für Polymerforschung.
‡ Université de Montréal.
§ Present address: Laboratoire de Stéréochimie et des Interactions Moléculaires, UMR-5532, CNRS/ENS, Ecole Normale Supérieure de Lyon, 69364 Lyon, France.

(1) Jeffrey, G. A.; Saenger, W. *Hydrogen Bonding in Biological Structures*; Springer-Verlag: New York, 1991.
(2) Gullion, T.; Schaefer, J. *Adv. Magn. Reson.* **1989**, *13*, 57.
(3) *Proceedings of "The Future of Solid State NMR in Biology" Conference*, Leiden, Netherlands, October 2000.
(4) (a) Feng, X.; Lee, Y. K.; Sandstrøm, D.; Edén, M.; Maisel, H.; Sebald, A.; Levitt, M. H. *Chem. Phys. Lett.* **1996**, *257*, 314. (b) Hong, M.; Gross, J. D.; Griffin, R. G. *J. Phys. Chem. B* **1997**, *101*, 5869.
(5) Jakobsen, H. J. In *Encyclopedia of Nuclear Magnetic Resonance*; Grant, D. M., Harris, R. K., Eds.; Wiley: Chichester, 1996; Vol. 1, p 398.
(6) Dec, S. F.; Bronnimann, C. E.; Wind, R. A.; Maciel, G. E. *J. Magn. Reson.* **1989**, *82*, 454.
(7) (a) Gerstein, B. C.; Chou, C.; Pembleton, R. G.; Wilson, R. C. *J. Phys. Chem.* **1977**, *81*, 565. (b) Scheler, G.; Haubenreisser, U.; Rosenberger, H. *J. Magn. Reson.* **1981**, *44*, 134.
(8) (a) Schnell, I.; Brown, S. P.; Low, H. Y.; Ishida, H.; Spiess, H. W. *J. Am. Chem. Soc.* **1998**, *120*, 11784. (b) Brown, S. P.; Schnell, I.; Brand, J. D.; Müllen, K.; Spiess, H. W. *J. Am. Chem. Soc.* **1999**, *121*, 6712. (c) Brown, S. P.; Schnell, I.; Brand, J. D.; Müllen, K.; Spiess, H. W. *J. Mol. Struct.* **2000**, *521*, 179. (d) Brown, S. P.; Schnell, I.; Brand, J. D.; Müllen, K.; Spiess, H. W. *Phys. Chem. Chem. Phys.* **2000**, *2*, 1735. (e) Brown, S. P.; Schaller, T.; Seelbach, U. P.; Koziol, F.; Ochsenfeld, C.; Klärner, F.-G.; Spiess, H. W. *Angew. Chem., Int. Ed. Engl.* **2001**, *40*, 717. (f) Rodriguez, L. N. J.; De Paul, S.; Barrett, C. J.; Reven, L.; Spiess, H. W. *Adv. Mater.* **2000**, *12*, 1934.
(9) Ishii, Y.; Tycko, R. *J. Magn. Reson.* **2000**, *142*, 199.
(10) Yamauchi, K.; Kuroki, S.; Fujii, K.; Ando, I. *Chem. Phys. Lett.* **2000**, *324*, 435.

10.1021/ja004231h CCC: $20.00
Published on Web 04/13/2001

strated that the semiquantitative information about specific proton−proton proximities yielded by rotor-synchronized two-dimensional ^{1}H DQ MAS spectra allows the differentiation between distinct hydrogen-bonding structures[8a] as well as the identification of particular aromatic $\pi-\pi$ packing arrangements.[8b,c] Moreover, an analysis of rotor-encoded ^{1}H DQ MAS spinning-sideband patterns[13] enables the quantitative determination of the internuclear distance for well-isolated proton−proton pairs in the solid phase as well as the order parameter in the liquid-crystalline phase.[8b] In this paper, our aim is to demonstrate the applicability of ^{1}H DQ MAS NMR spectroscopy to the quantitative investigation of the structure and geometry of a complex hydrogen-bonded arrangement, where the protons do not occur as well-isolated spin pairs.

Bilirubin

Bilirubin IXα (henceforth referred to simply as bilirubin), **1a**, is an unsymmetrically substituted tetrapyrrole dicarboxylic acid, which is found in the body as a product of the metabolism of hemoglobin from red blood cells.[14] Bilirubin itself is intrinsically unexcretable, and its removal from the body requires it first to be conjugated enzymatically with glucuronic acid in the liver. An insufficient elimination of the yellow-orange pigment, bilirubin, results in hyperbilirubinemia, which manifests itself as jaundice; such a condition is usually associated with a pathologic liver disease, e.g. hepatitis, or an insufficiency of the bilirubin glucuronyl transferase enzyme, the latter being commonly the case in newly born infants.[15]

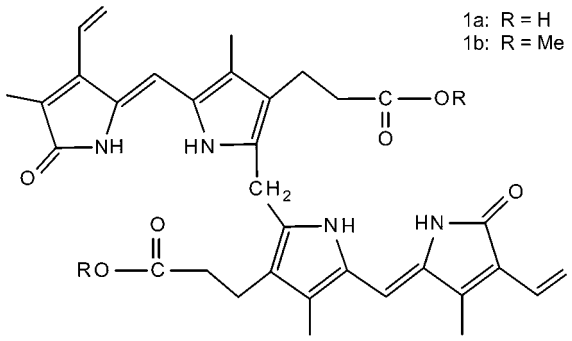

Because of its medical importance, much effort has been devoted to the investigation of the structure of bilirubin. X-ray single-crystal studies have demonstrated that bilirubin crystallizes in the solid state with the ridge-tile-shaped conformation illustrated in Figure 1—the two halves of the molecule can be considered to be planar tiles, aligned at an angle of approximately 100° with respect to each other.[16,17] Rotation is possible about the CH_2 group linking the two dipyrrinone units,

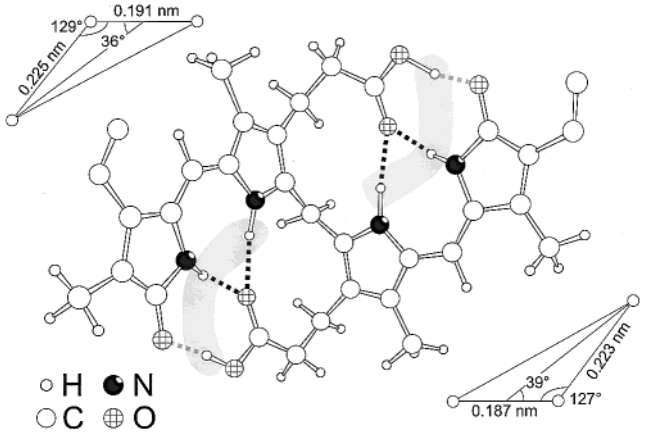

Figure 1. Structure adopted by bilirubin IXα in the solid state, as determined by an X-ray single-crystal diffraction study.[17] The intramolecular hydrogen-bonding arrangement is indicated. Oxygen, nitrogen, carbon, and hydrogen atoms are represented by hatched, black, large white, and small white circles, respectively. Note that, because of disorder among the alkene substituents, it was not possible to locate the alkene hydrogens. The insets show the arrangement of the three hydrogen-bonding protons for the two halves of the molecule.

with the result that the carboxyl acid group of one dipyrrinone unit can adopt an ideal geometry for intramolecular hydrogen bonding with the lactam and pyrrole moieties of the other dipyrrinone unit.[18] The involvement of the carboxylic acid groups in strong intramolecular hydrogen bonding renders bilirubin effectively insoluble in aqueous solution. The carboxylic acid to amide hydrogen-bonded arrangement found in bilirubin is surprisingly rare.[19] Bilirubin has also been extensively studied by solution-state NMR, from which it is known that bilirubin adopts the same conformation in a solution of chloroform as in the solid state.[20] In addition to ^{1}H and ^{13}C NMR, ^{15}N NMR experiments have also been carried out, which allow a clear assignment of the pyrrole and lactam resonances.[21] In addition to the investigation of bilirubin itself, attention has also been focused on the synthesis and characterization of bilirubin derivatives.[22]

In Figure 1, the distances between the hydrogen-bonded protons as well as their geometrical arrangement, as given by the X-ray single-crystal analysis reported by Le Bas et al.,[17] are specified. As stated above, the exact localization of protons by X-ray scattering is very difficult. Indeed, in the first X-ray single-crystal study,[16] the positions of the vital hydrogen-bonded protons were very poorly defined. Furthermore, although Le Bas et al. went to considerable trouble to obtain a single crystal of suitable quality to allow the location of the hydrogen-bonded protons, they were still forced to artificially calculate the position of one of the three hydrogen-bonded protons in each half of the bilirubin molecule.[17] Therefore, an alternative determination

(11) Ernst, R. R.; Bodenhausen, G.; Wokaun, A. *Principles of Nuclear Magnetic Resonance in One and Two Dimensions*; Clarendon: Oxford, 1987.

(12) Geen, H.; Titman, J. J.; Gottwald, J.; Spiess, H. W. *Chem. Phys. Lett.* **1994**, *227*, 79.

(13) (a) Geen, H.; Titman, J. J.; Gottwald, J.; Spiess, H. W. *J. Magn. Reson. A* **1995**, *114*, 264. (b) Gottwald, J.; Demco, D. E.; Graf, R.; Spiess, H. W. *Chem. Phys. Lett.* **1995**, *243*, 314.

(14) McDonagh, A. F. Bile Pigments: Bilatrienes and 5, 15-Biladienes. In *The Porphyrins*; Dolphin, D., Ed.; Acdemic Press: New York, 1979; Vol. VI, Chapter 6.

(15) (a) Schmid, R.; McDonagh, A. In *The metabolic basis of inherited diseases*; Stanbury, J. B., Wyngaarden, J. B., Frederickson, D. S., Eds.; McGraw-Hill: New York, 1978; pp 1221−1257. (b) Ostrow, J. D., Ed. *Bile Pigments and Jaundice*; Marcel-Dekker: New York, 1986. (c) Chowdhury, J. R.; Wolkoff, A. S.; Chowdhury, N. R.; Arias, I. M. In *The Metabolic and Molecular Bases of Inherited Diseases*; Scriver, C. R., Beaudet, A. L., Sly, W. S., Valle, D., Eds.; McGraw-Hill: New York, 1995; Vol. II, pp 2161−2208.

(16) Bonnett, R.; Davies, J. E.; Hursthouse, M. B. *Nature* **1976**, *262*, 326.

(17) Le Bas, G.; Allegret, A.; Mauguen, Y.; de Rango, C.; Bailly, M. *Acta Crystallogr.* **1980**, *B36*, 3007.

(18) Person, R. V.; Peterson, B. R.; Lightner, D. A. *J. Am. Chem. Soc.* **1994**, *116*, 42.

(19) (a) Boiadjiev, S. E.; Anstine, D. T.; Lightner, D. A. *J. Am. Chem. Soc.* **1995**, *117*, 8727. (b) Wash, P. L.; Maverick, E.; Chiefari, J.; Lightner, D. A. *J. Am. Chem. Soc.* **1997**, *119*, 3802.

(20) Kaplan, D.; Navon, G. *Isr. J. Chem.* **1983**, *23*, 177.

(21) Zhu, X. X.; Sauriol, F.; Brown, G. R. *Can. J. Spectrosc.* **1988**, *33*, 63.

(22) (a) Nogales, D.; Lightner, D. A. *J. Biol. Chem.* **1995**, *270*, 73. (b) Crusats, J.; Delgado, A.; Farrera, J.-A.; Rubires, R.; Ribó, J. M. *Monatsh. Chem.* **1998**, 129, *741*. (c) Chen, Q.; Huggins, M. T.; Lightner, D. A.; Norona, W.; McDonagh, A. F. *J. Am. Chem. Soc.* **1999**, *121*, 9253. (d) Huggins, M. T.; Lightner, D. A. *Tetrahedron* **2000**, *56*, 1797.

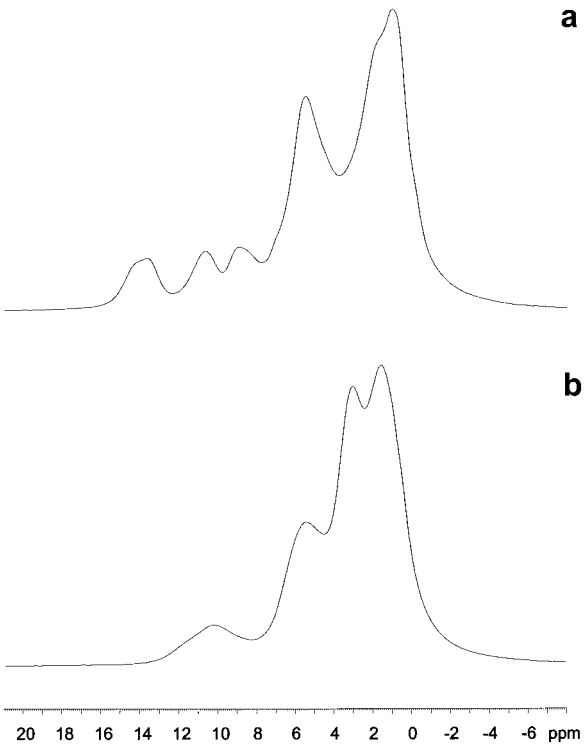

Figure 2. One-dimensional ^{1}H (700.1 MHz) MAS NMR spectra of (a) bilirubin, **1a**, and (b) its dimethyl ester, **1b**, recorded under MAS at 30 kHz.

of the proton positions by solid-state NMR is of particular interest.

Assigning the Hydrogen-Bonded Protons by Means of Specific H−H Proximities

Figure 2 presents ^{1}H MAS spectra of (a) bilirubin, **1a**, and (b) its dimethyl ester, **1b**, recorded at a ^{1}H Larmor frequency of 700.1 MHz and a MAS frequency of 30 kHz. Although the ^{1}H MAS line widths are still much greater than those observed in solution-state NMR, the resolution is sufficient to allow the clear identification of distinct resonances. It is well known that hydrogen bonding leads to marked downfield chemical shifts,[23] and thus the peaks above and below 8 ppm can be immediately assigned to hydrogen-bonded and aliphatic protons, respectively.

Considering the aliphatic region, there are resolved features at 1.0, 1.7 (a shoulder), and 5.6 ppm in Figure 2a, and at 1.6, 3.1, and 5.5 ppm in Figure 2b. To assign these peaks, it is informative to make a comparison with the solution-state chemical shifts.[20] However, some care must be adopted since, in the solid state, the through-space influence of nearby groups must be considered. In particular, it has recently been observed that the ring currents associated with aromatic moieties can lead to 2−3 ppm upfield changes in the experimental chemical shifts.[8b,c,e,24] Such effects of ring currents on NMR chemical shifts are, of course, well established;[25] however, it is only recently, with the development of solid-state NMR methods allowing the resolution of ^{1}H resonances, that the widespread importance of these effects in organic solids is gaining attention. Ab initio quantum chemical calculations show that these effects are particularly long range, with an aromatic ring still exerting an influence at a distance of 0.7 nm.[26] Despite these considerations, it is nevertheless reasonable to make the following assignments: first, the peaks at 5.5 and 5.6 ppm can be attributed to the alkene protons, while the new peak in Figure 2b at 3.1 ppm is most likely due to the methyl ester protons. The focus of this paper is the hydrogen-bonded protons, and we thus devote no further attention here to the identification and assignment of the particular aliphatic protons, which could easily be obtained by means of a two-dimensional ^{1}H−^{13}C correlation experiment.[27]

Figure 3 shows the regions corresponding to the hydrogen-bonded protons of rotor-synchronized ^{1}H (700.1 MHz) DQ MAS spectra[8a,c] recorded for (a) bilirubin and (b) its dimethyl ester at a MAS frequency of 30 kHz using one cycle (of duration one rotor period, τ_R) of the BABA[28] recoupling method for the excitation and reconversion of DQ coherence (DQC)—the pulse sequence and coherence transfer pathway diagram[29] are given in Figure 4. In such an experiment, the evolution of DQC among pairs of dipolar-coupled protons is observed in the indirect dimension (t_1)—note that the DQ frequency corresponding to a given DQC is simply the sum of the two single-quantum (SQ) frequencies. To interpret the spectra in Figure 3, it is simply necessary to remember that the presence of a given DQ peak implies a close proximity of the two involved protons, since both the excitation of a DQC and the subsequent reconversion to observable SQ coherence rely on the existence of a dipolar coupling between the two protons. For short recoupling times, the integrated intensity of the DQ peaks due to a particular DQC is proportional to D^2, where the dipolar coupling constant, D, is given by

$$D = \frac{(\mu_0/4\pi)\hbar\gamma_H^2}{r^3} \qquad (1)$$

and r is the internuclear distance.[30] Thus, from the relative intensities of the DQ peaks in a rotor-synchronized spectrum, semiquantitative information about relative proton−proton proximities is straightforwardly available.

Bilirubin. In the ^{1}H DQ MAS spectrum of bilirubin in Figure 3a, the DQ frequencies of the most intense DQ peaks, i.e., those due to DQCs involving solely the hydrogen-bonded protons, are indicated. Only the proton corresponding to the middle hydrogen-bonded peak at 10.8 ppm can then be seen to be in close proximity to both of the other hydrogen-bonded protons. By reference to the intramolecular hydrogen-bonded arrangement known from the single-crystal X-ray investigation (see Figure 1), the peak at 10.8 ppm can then be assigned to the lactam NH proton. From the DQ projection in Figure 3a, it is apparent that the pair of DQ peaks involving the SQ resonances at 10.8 and 9.1 ppm are significantly more intense than the other

(23) (a) Berglund, B.; Vaughan, R. W. *J. Chem. Phys.* **1980**, *73*, 2037. (b) Jeffrey, G. A.; Yeon, Y. *Acta Crystallogr.* **1986**, *B42*, 410. (c) Harris, R. K.; Jackson, P.; Merwin, L. H.; Say, B. J.; Hagele, G. *J. Chem. Soc., Faraday Trans.* **1988**, *84*, 3649.

(24) van Rossum, B.-J.; Boender, G. J.; Mulder, F. M.; Raap, J.; Balaban, T. S.; Holzwarth, A.; Schaffner, K.; Prytulla, S.; Oschkinat, H.; de Groot, H. J. M. *Spectrochim. Acta* **1998**, *A54*, 1167.

(25) Lazzeretti, P. *Prog. NMR Spectrosc.* **2000**, *36*, 1.

(26) Ochsenfeld, C.; Brown, S. P.; Schnell, I.; Gauss, J.; Spiess, H. W. *J. Am. Chem. Soc.* **2001,** *123*, 2597.

(27) (a) Van Rossum, B.-J.; Förster, H.; De Groot, H. J. M. *J. Magn. Reson.* 1996, *124*, 516. (b) Lesage, A.; Sakellariou, D.; Steuernagel, S.; Emsley, L. *J. Am. Chem. Soc.* **1998**, *120*, 13194. (c) Saalwächter, K.; Graf, R.; Spiess, H. W. *J. Magn. Reson.* **1999**, *140*, 471. (d) Saalwächter, K.; Graf, R.; Spiess, H. W. *J. Magn. Reson.* **2001**, *148*, 398.

(28) Sommer, W.; Gottwald, J.; Demco, D. E.; Spiess, H. W. *J. Magn. Reson. A* **1995**, *113*, 131.

(29) (a) Bodenhausen, G.; Kogler, H.; Ernst, R. R. *J. Magn. Reson.* **1984**, *58*, 370. (b) Hore, P. J.; Jones, J. A.; Wimperis, S. *NMR: The Toolokit*; Oxford University Press: Oxford, 2000; Chapter 6.

(30) (a) Graf, R.; Demco, D. E.; Gottwald, J.; Hafner, S.; Spiess, H. W. *J. Chem. Phys.* **1997**, *106*, 885. (b) Schnell, I.; Spiess, H. W. *J. Magn. Reson.* **2001**, in press.

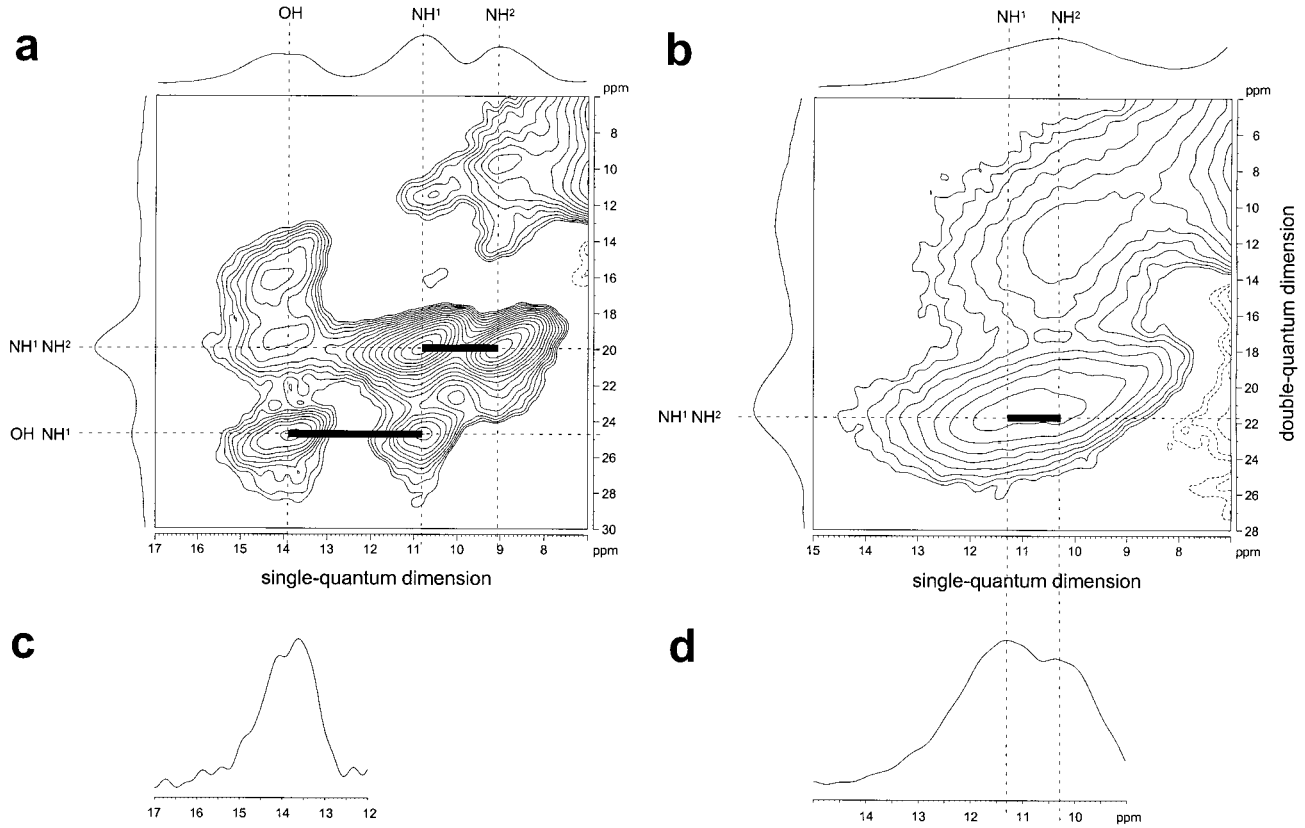

Figure 3. (a,b) The parts corresponding to the hydrogen-bonded resonances of rotor-synchronized ^{1}H (700.1 MHz) DQ MAS NMR spectra, together with skyline SQ and DQ projections, of (a) bilirubin, **1a**, and (b) its dimethyl ester, **1b**, recorded under MAS at 30 kHz using one cycle of the BABA recoupling sequence for the excitation and reconversion of DQCs. In the displayed spectral regions, there are no DQ peaks corresponding to DQCs between like spins, and it should be noted that, to allow a better centring of the spectral features, the diagonals do not correspond to the usual $\nu_1 = 2\nu_2$ convention adopted in previously published spectra. Note also that slightly different spectral regions are shown in (a) and (b). The assignment of the peaks is discussed in the text. DQ slices through (c) the OH NH^1 peak in (a) and (d) the NH^1 NH^2 peak in (b) are additionally shown.

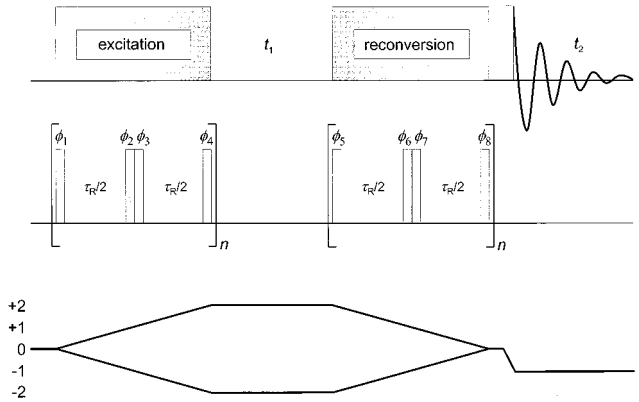

Figure 4. Pulse sequence and coherence transfer pathway diagram for a ^{1}H DQ MAS experiment using the BABA recoupling sequence for the excitation and reconversion of DQCs. The rectangular blocks represent pulses of flip angle 90°, with the choice of the phases $\phi_1-\phi_8$ being described in the Experimental Section. If the t_1 increment is set equal to a rotor period, a rotor-synchronized two-dimensional spectrum is obtained, while reducing t_1, and hence increasing the DQ spectral width, leads to the observation of a DQ MAS spinning-sideband pattern.

pair. As illustrated in Figure 1, the X-ray single-crystal structure due to Le Bas et al.[17] indicates that the lactam and pyrrole NH protons are closer together (0.187 and 0.191 nm) than the lactam NH and carboxylic acid OH protons (0.223 and 0.225 nm). On this basis, and considering the intensities of the respective DQ peaks, the SQ resonances at 9.1 and 13.9 ppm can be assigned to the pyrrole NH and carboxylic acid OH protons, respectively.

As stated above, there is strong evidence that the intramolecular hydrogen-bonding arrangement shown in Figure 1 persists in a solution of chloroform, and it is thus not surprising that there is a close agreement between the solid- and solution-state ^{1}H chemical shifts in that solvent, the latter (in ppm) being 9.27 and 9.29 (pyrrole NH), 10.68 and 10.79 (lactam NH), and 13.69 (carboxylic acid OH).[20]

Figure 3c presents the DQ slice corresponding to the COOH resonance, which appears to indicate the resolution of two maxima at 13.6 and 14.1 ppm. Possible explanations for this observation include slight variations in the hydrogen-bonding lengths, differing ring current effects associated with different packing arrangements for the two halves of the molecule, or alternatively a less than perfect crystallinity noted by Le Bas et al.[17]

The other DQ peaks at DQ frequencies (in ppm) of 19.5 and 15.8 (OH), 11.5 (lactam NH), and 14.1 and 9.8 (pyrrole NH) in Figure 3a correspond to DQCs between the hydrogen-bonded and aliphatic protons. Subtracting the chemical shift of the hydrogen-bonded proton in each case reveals that the aliphatic partners have SQ chemical shifts (in ppm) of 5.6 and 1.9 (OH), 0.7 (lactam NH), and 5.0 and 0.7 (pyrrole NH). As stated above, the observation of these DQ peaks indicates a close through-space proximity of the relevant two protons (less than 0.35 nm; see ref 30b). On the basis of the X-ray single-crystal structure,[17] for an isolated molecule, the only aliphatic proton within the required distance of a hydrogen-bonded proton is one of the bridging CH_2 protons, which is 0.251 nm away from the pyrrole NH. Considering intermolecular proximities, the lactam NH is

found to be only 0.252 nm away from the same CH_2 proton having an *intra*molecular proximity to the pyrrole NH. This is in agreement with the fact that the aliphatic proton chemical shift is the same for the relevant DQ peaks. For this CH_2 group, the ^{1}H SQ chemical shift of 0.7 ppm is much lower than the solution-state (chloroform) value of 4.08 ppm.[20] The marked difference is due to the crystal packing arrangement, in which the methylene proton under consideration is located above the pyrrole ring of the neighboring molecule, and is thus shielded on account of the ring current. In this respect, note that the intramolecular ring current due to the other pyrrole ring has been used to explain the low ^{1}H solution-state chemical shift of the hydrogen-bonded pyrrole NH.[31]

Furthermore, one of the CH_2 protons in an α position relative to a pyrrole ring has an intermolecular proximity of 0.281 nm to an OH proton.[17] The DQ peak at a DQ frequency of 15.8 ppm corresponds to this dipolar-coupled proton pair. The two remaining DQ peaks correlate the OH and pyrrole NH SQ resonances with aliphatic SQ peaks at 5.6 and 5.0 ppm, respectively. These DQ peaks, therefore, involve alkene protons. The disorder of the substituent alkene groups observed by Le Bas et al.,[17] however, precludes an assignment on the basis of the X-ray crystal structure. In this respect, the ^{1}H DQ MAS spectrum provides further useful information in demonstrating that the OH and pyrrole NH have a significantly closer intermolecular proximity to an alkene group than the lactam NH—it should be noted that a very weak peak at a DQ chemical shift of about 16 ppm is apparent for the lactam NH.

Bilirubin Dimethyl Ester. In bilirubin dimethyl ester, **1b**, the COOH proton is no longer present, and thus there are only two different protons capable of hydrogen bonding. To the best of our knowledge, no single-crystal structural data are available for this molecule. Unlike in the case of bilirubin, there is no clear resolution of distinct hydrogen-bonded peaks in the one-dimensional spectrum (see Figure 2b). However, as shown in Figure 3b, the presence of two distinct NH resonances is evident in the ^{1}H DQ MAS spectrum: the DQ peak at 21.6 ppm is due to the proximity of two NH protons at 10.3 and 11.3 ppm (see the DQ slice in Figure 3d). It is thus apparent that the NH chemical shifts, in particular the lower value, are quite different from the bilirubin case, which demonstrates the importance of the COOH proton to the hydrogen-bonding arrangement adopted by the NH protons in bilirubin. A comparison of the solid- and solution-state ($CDCl_3$) chemical shifts, the latter being 10.18 and 10.49 (pyrrole NH) and 11.23 and 10.10 (lactam NH),[20] again reveals a close similarity.

The ^{1}H DQ MAS spectrum in Figure 3b also provides information about the proximity of the NH protons to aliphatic protons. Focusing on the part of the spectrum corresponding to DQCs between NH and aliphatic protons, a broad peak centered at SQ and DQ frequencies of 10.3 and 11.3 ppm, respectively, is observed. It is thus apparent that the NH proton with the lower chemical shift has a significantly closer proximity to an alkyl proton (with a chemical shift of 1.0 ppm) than the other NH proton. The broadness of this resonance, however, indicates that there are other relatively close proximities between the NH protons and other aliphatic protons.

The Quantitative Determination of Proton−Proton Distances and Geometry

The Strategy: The Initial Estimation of the Shortest Proton−Proton Distance. Rotor-synchronized ^{1}H DQ MAS spectra can only deliver information about relative proton−proton proximities (except for cases in which the DQ peak(s) due to a known internal or external standard are well resolved).[30b] The DQ MAS experiment (see Figure 4) can, however, be performed in an alternative fashion: if the t_1 increment is reduced, which corresponds to an increase in the DQ spectral width, a DQ MAS spinning-sideband pattern is observed[8b,c] (provided that a recoupling sequence which has an amplitude dependence on the rotor phase, e.g., BABA[28] or DRAMA,[32] is used). For an isolated spin pair, the sole means by which spinning sidebands arise is the so-called reconversion rotor encoding (RRE) mechanism.[13,33] The resulting patterns are very sensitive to the product of D and the recoupling time, τ_{rcpl}. For the well-isolated pairs of aromatic protons in a hexabenzocoronene derivative, the ability to quantitatively determine the internuclear separation for the solid phase as well as the order parameter of the liquid-crystalline phase by an analysis of ^{1}H DQ MAS spinning-sideband patterns has been clearly demonstrated.[8b] In this paper, we show that an analysis of ^{1}H DQ MAS spinning-sideband patterns obtained for the three-spin hydrogen-bonding arrangement in bilirubin allows the determination of dipolar couplings, and hence proton−proton distances, as well as the relative geometry of the spins, even though the pairs of protons which give rise to observed DQCs are clearly not well isolated. First, we must justify the validity of our approach.

Consider a model isosceles triangle three-spin system, where the distances between spins A and B, A and C, and B and C are 0.198, 0.238, and 0.238 nm, respectively, corresponding to $D/2\pi$ values of 15.5, 8.9, and 8.9 kHz. Spins A and B, which participate in the strongest dipolar coupling, are on resonance, while spin C is 4 kHz off resonance, such that the sideband patterns due to the distinct DQCs can be resolved. Using these parameters, three-spin explicit density matrix simulations were performed, further assuming that all radio frequency pulses are infinitely short. In Figure 5a−c, ^{1}H DQ MAS spinning-sideband patterns for uncompensated BABA recoupling sequences of duration one, two, and four rotor periods at MAS frequencies of 15, 30, and 60 kHz in (a), (b), and (c), respectively, are presented. The sideband patterns are detected at spin B; in this way, for each sideband order, the left- and right-hand peaks correspond to DQCs between spins B and C and between spins A and B, respectively. The same line broadening (2 kHz) was applied in each case, and the narrowing of the lines is a consequence of the fact that the displayed spectral width (in kilohertz) doubles on going from (a) to (b) and from (b) to (c). Some phase distortions are observed for the sidebands due to the BC DQC on account of the off-resonance excitation. For comparison, Figure 5d,e presents spectra generated for a BABA recoupling sequence of duration two rotor periods at a MAS frequency of 30 kHz using the analytical time domain formula for an isolated spin pair,[8b,30a] with $D/2\pi$ values of (d) 8.9 and (e) 15.5 kHz, i.e., corresponding to the perturbing (BC) and dominant (AB) couplings in the model system.

In the spectra for an isolated spin pair (Figure 5d,e), only odd-order spinning sidebands are present—this is a characteristic feature of the RRE mechanism.[33] Note also the significant changes in the relative intensities of the observed spinning sidebands upon increasing D. For the three-spin simulation at a MAS frequency of 15 kHz (Figure 5a), significant intensity at the center band and even-order spinning-sideband positions is observed. The presence of these peaks arises from the evolution during t_1 of a DQC, due to a particular two spins, under dipolar couplings to other spins; this mechanism, by

(31) Tipton, A. K.; Lightner, D. A. *Monatsh. Chem.* **1999**, *130*, 425.

(32) Tycko, R.; Dabbagh, G. *J. Am. Chem. Soc.* **1991**, *113*, 9444.

(33) Friedrich, U.; Schnell, I.; Brown, S. P.; Lupulescu, A.; Demco, D. E.; Spiess, H. W. *Mol. Phys.* **1998**, *95*, 1209.

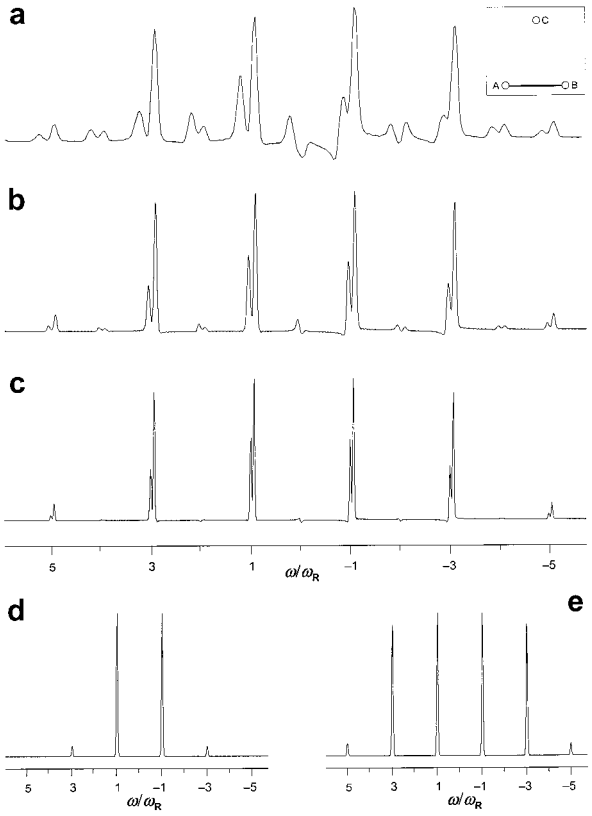

Figure 5. (a−c) Simulated ^{1}H DQ MAS spinning-sideband patterns for an isosceles triangle arrangement of three spins, where the $D/2\pi$ values for spins A and B, A and C, and B and C are 15.5, 8.9, and 8.9 kHz (corresponding to distances of 0.198, 0.238, and 0.238 nm), respectively. Spins A and B are on resonance, while spin C is 4 kHz off resonance. The sideband patterns are detected at spin B; in this way, for each sideband order, the left- and right-hand peaks correspond to DQCs between spins B and C and A and B, respectively. Numerical density matrix simulations, assuming infinitely short radio frequency pulses, were performed for uncompensated BABA recoupling sequences ($\bar{X}\,\bar{X}\,Y\,\bar{Y}$) of duration one, two, and four rotor periods at MAS frequencies of 15, 30, and 60 kHz in (a), (b), and (c), respectively. (d,e) Spectra generated using the analytical time domain formula for an isolated spin pair,[8b,30a] with $D/2\pi$ values of (d) 8.9 and (e) 15.5 kHz, for a BABA recoupling sequence of duration two rotor periods at a MAS frequency of 30 kHz. The same Gaussian line-broadening was applied for all spectra.

means of which spinning sidebands are, in fact, most commonly generated, may be termed evolution rotor modulation.[33] Recently, Shantz et al. have shown how the observation of such sidebands in a ^{1}H DQ MAS spectrum proves that at least three silanol protons are engaged in hydrogen bonding within the defect sites in an all-silica ZSM-12 zeolite.[34] On increasing the MAS frequency from 15 to 30 to 60 kHz, the intensity of the center band and even-order spinning-sideband peaks is observed to decrease. During t_1, no recoupling pulse sequence is applied, and the averaging of the dipolar couplings to zero becomes ever more efficient upon increasing the MAS frequency, such that there is a virtual absence of center band and even-order sideband intensity in Figure 5c.

During the excitation and reconversion of DQCs, the BABA recoupling sequence is applied, which acts against the averaging to zero of the dipolar couplings by MAS. Since the origin of the RRE mechanism is the change in the Hamiltonian active during the DQ reconversion period relative to the excitation period,[33] it is to be expected that the observed odd-order sideband pattern is dependent on the perturbing dipolar couplings in a multispin system. Comparing the isolated spin-pair analytical spectra (Figure 5d,e) to the two sideband patterns in Figure 5c, it is apparent that, while the patterns for the DQC with the weaker dipolar coupling constant are quite different, i.e., the third-order sidebands are much higher in the three-spin system, the pattern for the dominant coupling in the three-spin system is only slightly different from that for the isolated spin pair. It is also important to note that the odd-order sideband pattern is virtually unchanged on doubling the MAS frequency from 30 to 60 kHz—the only change is the loss of the slight asymmetry in the first-order sidebands due to the perturbing coupling in Figure 5c. Therefore, a MAS frequency of 30 kHz suffices, as far as the determination of the limiting ^{1}H DQ MAS sideband pattern is concerned;[30b,35] a higher MAS frequency, though, would lead to better resolution, provided that the line broadening is due to residual dipolar couplings rather than an inherent distribution of chemical shifts.

The above simulations have demonstrated, for a multispin system, that an analysis based on the assumption of an isolated spin pair yields a reasonably accurate D for the dominant coupling, hence allowing a good estimation of the shortest proton−proton distance. Thus, such an analysis represents the first step in our strategy for extracting distance and geometry information from ^{1}H DQ MAS spinning-sideband patterns. In this respect, it should be emphasized that it is important to extract, by means of a line-shape analysis of the experimental spectra, the integrated intensity for each sideband. In the following, a refinement of the analysis procedure is outlined, which involves performing three-spin density matrix simulations, taking into account the experimentally used parameters (i.e., finite 90° pulse lengths, finite delays between pulses, and resonance offsets) and considering different geometrical arrangements of the three protons.

The Strategy: The Refinement. It is known that the geometrical arrangement in a multispin system affects the observed ^{1}H DQ MAS spinning-sideband pattern.[30b] Thus, to investigate the effect of geometry in a three-spin system upon both rotor-synchronized DQ MAS spectra and DQ MAS spinning-sideband patterns, three-spin density matrix simulations were performed (these are described in the Supporting Information). Consideration of these simulations leads to the following protocol for the extraction of the absolute value of the dominant $D/2\pi$ (and hence the shortest proton−proton distance). ^{1}H DQ MAS spinning-sideband patterns are first simulated for a chosen θ, defined by the vector linking the midpoint of the internuclear vector AB with C, using the relative dominant and perturbing $D/2\pi$ values determined from an analysis of the rotor-synchronized spectrum, and choosing dominant $D/2\pi$ values in steps of 0.5 kHz within a range based upon the value determined by the analysis assuming an isolated spin pair. Comparing the extracted experimental sideband intensities with those of the simulated patterns, a best fit is determined according to a criterion which places a particular bias on the correct fitting of the highest-order sideband intensity. In a final refinement, the angle θ is varied in steps of 2.5°, and the best-fit spectrum is determined according to a minimization of the normalized squared deviation, $\epsilon^2 = \sum[I_{sim}(n) - I_{exp}(n)]^2/\sum I_{exp}(n)^2$, where $I_{sim}(n)$ and $I_{exp}(n)$ are the intensities of the nth point in the "extracted" simulated and experimental spectra—in such spectra, all peaks are represented by Gaussian lines of the same line width, with the peak height representing the integrated intensity.

(34) Shantz, D. F.; Schmedt auf der Günne, J.; Koller, H.; Lobo, R. F. *J. Am. Chem. Soc.* **2000**, *122*, 6659.

(35) Filip, C.; Hafner, S.; Schnell, I.; Demco, D. E.; Spiess, H. W. *J. Chem. Phys.* **1999**, *110*, 423.

The Strategy: The Uncertainty in the Extracted Parameters. To estimate the uncertainty inherent to our approach, it is necessary to consider the factors which are neglected. First, all simulations assume that the flip angle of each pulse has the ideal value of 90°. Experimentally, B_1 inhomogeneity means that there are regions of the sample where this is not the case, even when the flip angles are carefully calibrated. Simulations show that small deviations in the flip angle from 90° lead to small changes in the observed spinning-sideband patterns. In addition, further nearby protons external to the considered three-spin system will also perturb the observed sideband pattern. Third, the chemical shift anisotropy (CSA) of the hydrogen-bonded protons has not been considered in the above analysis. At a ^{1}H Larmor frequency of 700 MHz, the CSA anisotropy parameter for hydrogen-bonded protons is non-negligible, being approximately 10 kHz. Indeed, Tekeley et al. have shown that the CSA is responsible for distortions in the ^{1}H (300.1 MHz) DQ MAS spinning-sideband spectra obtained for barium chlorate monohydrate, $BaClO_3 \cdot H_2O$, with an excitation time of $\tau_R/2$.[36] However, these distortions manifest themselves mostly only in terms of a marked asymmetry of the lower-order sideband intensities, with the ratios of the average sideband intensities (e.g., first:third) being virtually unchanged. Furthermore, De Paul et al. have shown that including the CSA has only a minor effect on sideband patterns simulated for related rotor-encoded longitudinal magnetization (RELM) experiments, which also use BABA recoupling.[37] It should be noted that De Paul et al. have further shown that the situation is much less favorable for cases where the CSA is significantly bigger than the dipolar coupling, e.g., for ^{31}P.

Considering all these factors, it can be concluded that the uncertainty in the determination of the dominant coupling is small, being of the order of ±0.5 kHz. Therefore, an analysis of ^{1}H DQ MAS spinning-sideband patterns allows the shortest proton−proton distance in a multispin system to be measured to a typical accuracy of ±0.002 nm. Even where no information about the geometrical arrangement is known, the maximum possible error in the determination of the dominant coupling is unlikely to exceed ±1.0 kHz, corresponding to a typical error in the distance of only ±0.005 nm. We note that, at this degree of accuracy, the different effects of vibrational averaging should be considered when comparing distances extracted by solid-state NMR to those determined by neutron diffraction studies.[38]

Since the CSA primarily alters the intensities of the same sidebands which are sensitive to the geometry, the neglect of the CSA for hydrogen-bonded protons means that the accuracy in the determination of θ is, however, likely to be much worse. A reliable determination of the geometry would require a knowledge of the ^{1}H CSA tensors and their relative orientations, or the development of a new DQ recoupling scheme which is insensitive to CSAs. In this latter respect, Carravetta et al. have recently suggested sequences based on the R N_n^v symmetry which satisfy these criteria.[39] These sequences have not, however, been experimentally demonstrated, and a significant problem is likely to be the requirement for the sequence to function at 30 kHz.

Finally, we note that the simulated sideband patterns are found to be relatively insensitive to the magnitude of the perturbing coupling. This observation is in agreement with the findings of Hodgkinson and Emsley, who concluded that the measurements of medium- to long-range C−C distances in fully labeled ^{13}C systems, i.e., the determination of a small perturbing $D/2\pi$ in the presence of a dominant $D/2\pi$ between two directly bonded ^{13}C nuclei, using homonuclear recoupling methods is prone to large errors.[40] It should be remembered that in our case, i.e., the arrangement of three hydrogen-bonded protons, the determination of the dominant coupling and hence the shortest proton−proton distance, for which the accuracy is high, is of much interest, unlike the case above, where C−C bond lengths are well known. Concerning the perturbing coupling and hence the longer proton−proton distance, the uncertainty is that inherent to the analysis of the rotor-synchronized spectrum.

Bilirubin. ^{1}H (700.1 MHz) DQ MAS spinning-sideband patterns obtained for (a,c,e), the pyrrole (at 9.1 ppm) and (b,d,f), the lactam (at 10.8 ppm) NH resonances of bilirubin are shown in Figure 6. The spectra were recorded with τ_{rcpl} equal to 2 (a,b), 3 (c,d), and 4 (e,f) rotor periods, which corresponds to 67, 100, and 133 μs, respectively. It is then apparent that increasing τ_{rcpl}, and hence the product $D\tau_{rcpl}$, causes the signal to be distributed into spinning sidebands of increasing order. In the rotor-synchronized ^{1}H DQ MAS spectrum in Figure 3a, in addition to the intense NH−NH DQ peaks, weaker DQ peaks due to DQCs between the NH and aliphatic protons as well as between the lactam NH and OH protons are observed. An inspection of the spectra in Figure 6 reveals the existence of spinning sidebands due to all these different DQCs—see, in particular, the first-order spinning sidebands in Figure 6a,b (note that the DQ peak for the NH−NH pair is at the most left-hand and the second-to-left position in Figure 6a and 6b, respectively). It is evident that the highest-order spinning sidebands are observed only for the NH−NH pair. This immediately indicates, in agreement with the above discussion of the rotor-synchronized ^{1}H DQ MAS spectrum, that the dipolar coupling is the largest, and hence the proton−proton distance is the shortest, in this case. From the above discussion, we can therefore expect to be able to extract this distance with the highest degree of accuracy.

Spectra, simulated assuming an isolated proton pair,[8b,30] corresponding to a best-fit of the integrated intensities of the experimental odd-order spinning sidebands due to the NH−NH DQC are also shown in Figure 6 as dashed lines, displaced to the left of the experimental peaks. To ensure a good fit of the highest-order spinning sidebands, it was necessary to neglect the first-order sideband intensities in (c) and (d) and the first- and third-order sideband intensities in (e) and (f)—as discussed above, these sidebands are most prone to distortions due to the CSA. In this way, there were two parameters to be fit in each case, namely the following ratios of sideband intensities: (b) fifth:third and third:first, (d) seventh:fifth and fifth:third, and (f) ninth:seventh and seventh:fifth. The $D/2\pi$ values and internuclear distances corresponding to the simulated spectra are also given in Figure 6. The extracted $D/2\pi$ values and NH−NH distances are consistent with each other to within ±0.7 kHz and ±0.003 nm. Following the refinement protocol outlined above, we consider a three-spin system including the dipolar coupling of the lactam NH to the carboxylic acid proton as the perturbing coupling. In this way, we restrict our focus to the sideband patterns detected at the lactam NH resonance (i.e., Figure 6b,d,f). It should be noted that the analysis will return a single value for the two distances and one angle defining the

(36) Tekeley, P.; Demco, D. E.; Canet, D.; Malveau, C. *Chem. Phys. Lett.* **1999**, *309*, 101.

(37) De Paul, S. D.; Saalwächter, K.; Graf, R.; Spiess, H. W. *J. Magn. Reson.* **2000**, *146*, 140.

(38) (a) Henry, E. R.; Szabo, A. *J. Chem. Phys.* **1985**, *82*, 4753. (b) Roberts, J. E.; Harbison, G. S.; Munowitz, M. G.; Herzfeld, J.; Griffin, R. G. *J. Am. Chem. Soc.* **1987**, *109*, 4163.

(39) Carravetta, M.; Edén, M.; Zhao, X.; Brinkmann, A.; Levitt, M. H. *Chem. Phys. Lett.* **2000**, *321*, 205.

(40) Hodgkinson, P.; Emsley, L. *J. Magn. Reson.* **1999**, *139*, 46.

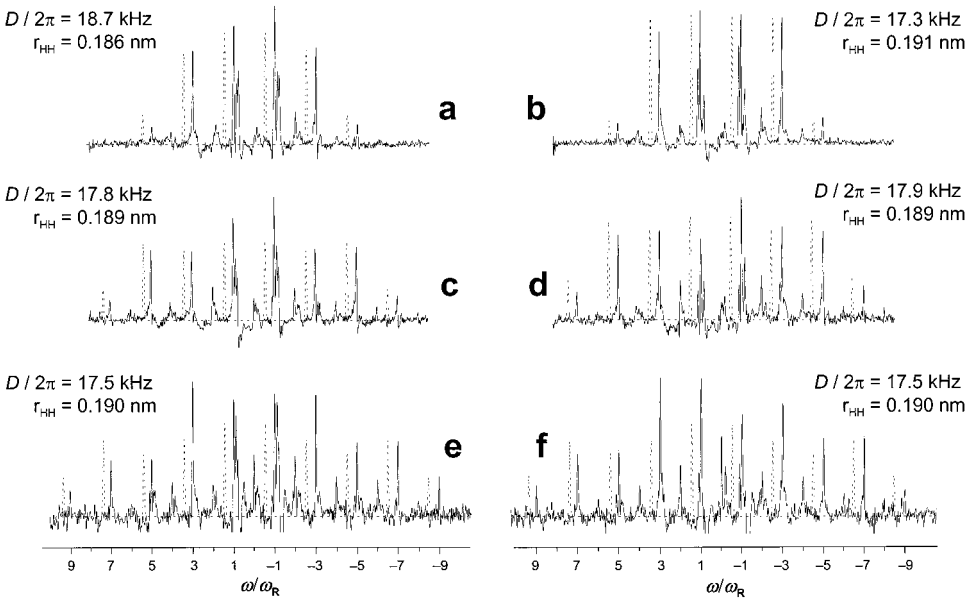

Figure 6. ^{1}H (700.1 MHz) DQ MAS NMR spinning-sideband patterns obtained for (a,c,e) the NH^2 and (b,d,f) the NH^1 hydrogen-bonded resonances of bilirubin (see Figure 3a) at a MAS frequency of 30 kHz. BABA recoupling sequences of duration two (a,b), three (c,d), or four (e,f) rotor periods were used for the excitation and reconversion of DQCs. The dashed lines, displaced to the left of the experimental spectra, correspond to spectra, generated using the analytical time domain formula for an isolated spin pair,[8b,30a] obtained from a fitting of the extracted experimental integrated sideband intensities; the corresponding $D/2\pi$ values and internuclear distances are indicated.

three-spin system—if there are differences between the two halves of the bilirubin molecule, the average values for the two arrangements will be determined.

As an initial estimation of the geometry, we use the average value of θ for the two halves of the molecule given by the X-ray single-crystal structure[17] (see Figure 1), i.e., 37.5°. For the rotor-synchronized ^{1}H DQ MAS spectrum in Figure 3a, a line shape analysis reveals that the integrated intensities of the two DQ peaks at the SQ frequency of the NH^1 proton are in the ratio of 0.38 ± 0.05. According to the protocol outlined above, in the first step, pairs of NH−OH and NH−NH $D/2\pi$ values which are consistent with this experimental rotor-synchronized spectrum are determined by means of three-spin density matrix simulations.

As the next step, ^{1}H DQ MAS spinning-sideband patterns were simulated using the parameters corresponding to the experimental spectra in Figure 6b,d,f. In the first stage, simulations were performed for NH−NH $D/2\pi$ values between 16.0 and 19.0 kHz (corresponding to H−H distances between 0.196 and 0.185 nm), in steps of 0.5 kHz, with $\theta = 37.5°$. For each NH−NH $D/2\pi$ value, the NH−OH $D/2\pi$ value was determined by analysis of the rotor-synchronized spectrum mentioned above. For the likely range of θ, the relative intensity of the highest-order sidebands is expected to be geometry independent (see Supporting Information). Thus, the best-fit NH−NH $D/2\pi$ was determined in each case by comparison of the simulated sideband intensities with the integrated intensities extracted from the experimental spectrum, which placed a particular bias on the correct fitting of the highest-order sidebands. In the final step, different values of θ between 30° and 45°, in steps of 2.5°, were considered to determine the best-fit of the lower-order spinning sidebands. With respect to the experimental spectra, we observed that the first-order spinning sidebands were slightly narrower than the higher-order sidebands. It is interesting to note that an analogous effect has been observed in ^{1}H SQ MAS spectra of adamantane where, in this case, the center band is noticeably narrower than the sidebands—this phenomenon has been explained on the basis of the increasing weight of higher spin correlations in the moments (i.e., line widths) of sidebands of increasing order.[30b,35]

To illustrate the marked sensitivity of the ^{1}H DQ MAS spinning-sideband pattern to the magnitude of the NH−NH $D/2\pi$ value, Figure 7 presents spectra simulated with a compensated BABA recoupling sequence of duration two rotor periods at a MAS frequency of 30 kHz for NH−NH $D/2\pi$ values of (a) 16.0, (b) 17.5, and (c) 19.0 kHz (the corresponding NH−NH distances are (a) 0.196, (b) 0.190, and (c) 0.185 nm) with $\theta = 37.5°$. The first-order sidebands have some dispersive character on account of the off-resonance excitation; similar small phase distortions are also apparent in the experimental spectra in Figure 6. Within each sideband order, the left- and right-hand peaks correspond to the NH−OH and NH−NH DQCs, respectively. Focusing first on the peaks due to the NH−NH DQC, the fifth-order sidebands grow in intensity from 8% in (a) to 23% in (c), as measured relative to the most intense sideband. In addition, it is apparent in (a) and (b) that the third-order sidebands are more intense than the first-order ones, while in (c) they are of similar height. Moreover, it is interesting to consider the relative heights of the first-order sidebands due to the NH−OH and NH−NH DQCs: in (a) those due to the NH−OH DQC are more intense, while in (c) they reach only about 60% of those due to the NH−NH DQC.

In Figure 8, the best-fit simulated three-spin ^{1}H DQ MAS spinning-sideband patterns for τ_{rcpl} equal to $2\tau_R$ and $3\tau_R$ are presented together with the corresponding experimental spectra. The extracted parameters are given in Table 1, from which it is seen that the fitting procedure delivered exactly the same parameters for these two experimental spectra, namely NH−NH and NH−OH $D/2\pi$ values of 18.5 ± 0.5 and 9.9 ± 1.0 kHz, respectively, corresponding to NH−NH and NH−OH distances of 0.186 ± 0.002 and 0.230 ± 0.008 nm, with a geometry given by $\theta = 42.5° \pm 2.5°$, which corresponds to a H−H−H angle of $122° \pm 4°$. As discussed above, a particular emphasis is placed on the correct fitting of the highest-order spinning-sidebands, but how good a fit is obtained for the other sideband orders? First, following the above discussion of

Table 1. Extracted Parameters for the Hydrogen-Bonded Arrangement in Bilirubin As Determined from an Analysis of ^{1}H DQ MAS Spinning-Sideband Patterns

	$(D/2\pi)$/kHz		H−H distance/nm				
τ_{rcpl}/τ_R	NH−NH	NH−OH	NH−NH	NH−OH	angle θ/deg	angle H−H−H/deg	normalized squared deviation
2	18.5 ± 0.5	9.9 ± 1.0	0.186 ± 0.002	0.230 ± 0.008	42.5 ± 2.5	122 ± 4	0.0028
3	18.5 ± 0.5	9.9 ± 1.0	0.186 ± 0.002	0.230 ± 0.008	42.5 ± 2.5	122 ± 4	0.0490
(4	17.5 ± 1.5	9.5 ± 2.0	0.190 ± 0.006	0.233 ± 0.019	37.5 ± 7.5	128 ± 10	0.1100**)**

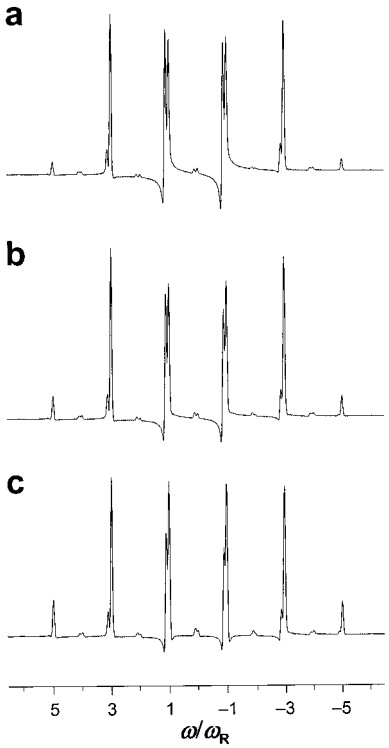

Figure 7. Simulated ^{1}H DQ MAS spinning-sideband patterns, detected at spin B (corresponding to NH^1 in Figure 3a), for three-spin systems based on the geometry, as determined by an X-ray single-crystal diffraction study,[17] of the OH, NH^1, and NH^2 hydrogen-bonded protons in bilirubin, i.e., $\theta = 37.5°$. The numerical density matrix simulations used the experimental parameters associated with the ^{1}H DQ MAS spinning-sideband pattern in Figure 6b, which was recorded with a compensated BABA recoupling sequence of duration two rotor periods at a MAS frequency of 30 kHz. The spectra were simulated for NH−NH $D/2\pi$ values of (a) 16.0, (b) 17.5, and (c) 19.0 kHz, corresponding to NH−NH distances of (a) 0.196, (b) 0.190, and (c) 0.185 nm. The NH−OH $D/2\pi$ values, as determined by an analysis of the rotor-synchronized spectrum as described in the text, are (a) 9.2, (b) 9.5, and (c) 10.0 kHz, corresponding to NH−OH distances of (a) 0.235, (b) 0.233, and (c) 0.229 nm.

Figure 7, we note a good agreement for the relative intensities of the sidebands due to the NH−OH DQC. By optimizing θ, a reasonable best-fit for the lower-order sidebands was achieved, considering, as stated above, that our analysis neglects the ^{1}H CSA, and thus a correct fitting of the experimentally observed asymmetry cannot be expected.

For the ^{1}H DQ MAS spinning-sideband patterns recorded with τ_{rcpl} equal to $4\tau_R$ (Figure 6f), it was not possible to obtain a good-quality fit. Therefore, the parameters listed in Table 1, which correspond to the simulated pattern in which the ninth-order sideband intensities best match the experimental spectrum, are put in parentheses and the given uncertainties are greater. Possible reasons for the poor fitting of this spectrum are the lower signal-to-noise ratio and the influence of other nearby protons becoming more significant for the longer recoupling time. Despite the inability to obtain a good-quality fit, this spectrum does not cast doubt on the reliability of the analysis for the spectra recorded with τ_{rcpl} equal to $2\tau_R$ and $3\tau_R$; for example, the fit to the analytical spin-pair formula in Figure 6f gives a consistent value for the NH−NH $D/2\pi$.

In the above discussion, in quoting H−H distances corresponding to the extracted dipolar couplings, we assume that no exchange of the positions of the hydrogen-bonded protons occurs for the following reasons: First, hydrogen exchange by proton tunneling, which occurs between the two tautomeric forms of a carboxylic acid dimer,[41] cannot occur in bilirubin because of the lack of symmetry.[1] Second, the type of intramolecular hydrogen bond exchange dynamics extensively investigated by Limbach and co-workers using ^{15}N solid-state NMR, e.g., in *N*,*N*-bisarylformamidines[42] or a phenylenediamine,[43] can be excluded for bilirubin since the tautomerism of the lactam group would lead to a particularly unstable C(OH)═N moiety. Thus, apart from the usual vibrational averaging inherent to any bond, our assumption of a rigid hydrogen-bonding structure seems justified. Slight changes in the ^{1}H chemical shifts upon heating are discussed in the Supporting Information.

The Dimethyl Ester of Bilirubin. In Figure 9, the ^{1}H (700.1 MHz) DQ MAS spinning-sideband patterns obtained for (a) the lactam NH in bilirubin (repeated from Figure 6d) and (c) the NH protons in dimethyl ester of bilirubin using $\tau_{rcpl} = 3\tau_R$ at a MAS frequency of 30 kHz are presented. A comparison of the extracted intensities for the sidebands due to the NH−NH DQCs (the solid lines in Figures 6b and 8d) immediately indicates that the $D/2\pi$ is bigger for bilirubin—the maximum sideband order is seven and five in Figure 9b and 9d, respectively. A fit (the dotted line in Figure 6d) of the extracted experimental intensities for the dimethyl ester to analytical spectra generated assuming an isolated spin pair[8b,30a] yields a NH−NH $D/2\pi$ of 13.5 kHz, corresponding to an H−H distance of 0.207 nm. Although the poor resolution means that this analysis is prone to a significant uncertainty, it is indisputable that the NH−NH distance is significantly longer than that in bilirubin.

Discussion

We have demonstrated that an analysis of ^{1}H DQ MAS spinning-sideband patterns allows the distance between the lactam and pyrrole NH protons within the complex hydrogen-bonding arrangement in bilirubin to be determined to an accuracy of ±0.002 nm. Such an accuracy is better than can be reliably expected from a standard X-ray structural analysis. It is to be emphasized that there was no requirement for synthetically demanding isotopic labeling, and only 10 mg of a powdered sample was needed. Importantly, this work has proven that, as long as the individual resonances are resolved, reliable distance measurements can be obtained for multispin systems where the protons do not exist as well-isolated spin pairs. For

(41) Stöckli, A.; Meier, B. H.; Kreis, R.; Meyer, R.; Ernst, R. R. *J. Chem. Phys.* **1990**, *93*, 1502.
(42) Anulewicz, R.; Wawer, I.; Krygowski, T. M.; Männle, F.; Limbach H.-H. *J. Am. Chem. Soc.* **1997**, *119*, 12223.
(43) Takeda, S.; Inabe, T.; Benedict, C.; Langer, U.; Limbach, H.-H. *Ber. Bunsen-Ges. Phys. Chem.* **1998**, *102*, 1358.

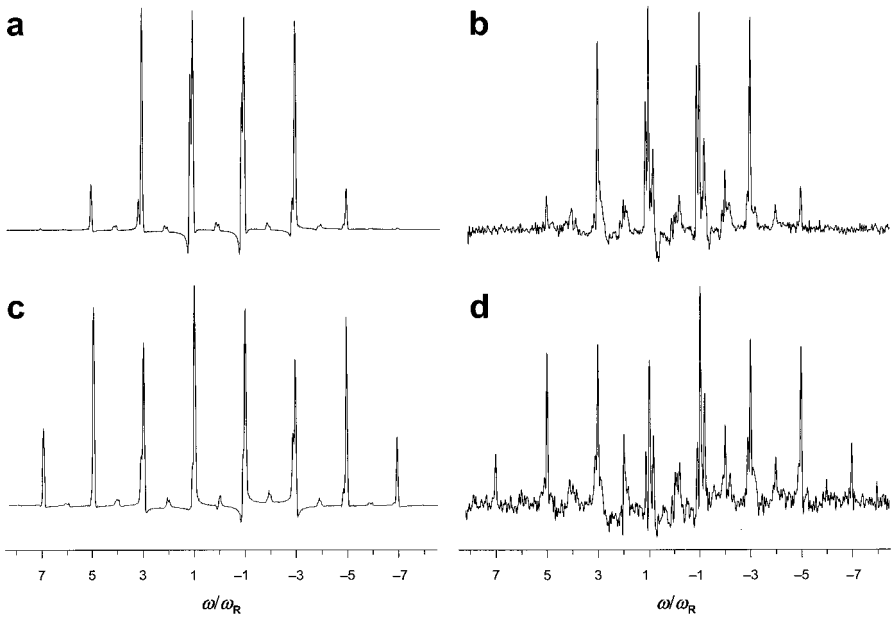

Figure 8. Best-fit simulated three-spin ^{1}H DQ MAS spinning-sideband patterns for τ_{rcpl} equal to (a) $2\tau_R$ and (c) $3\tau_R$, together with (b,d) the corresponding experimental spectra. The extracted parameters are given in Table 1.

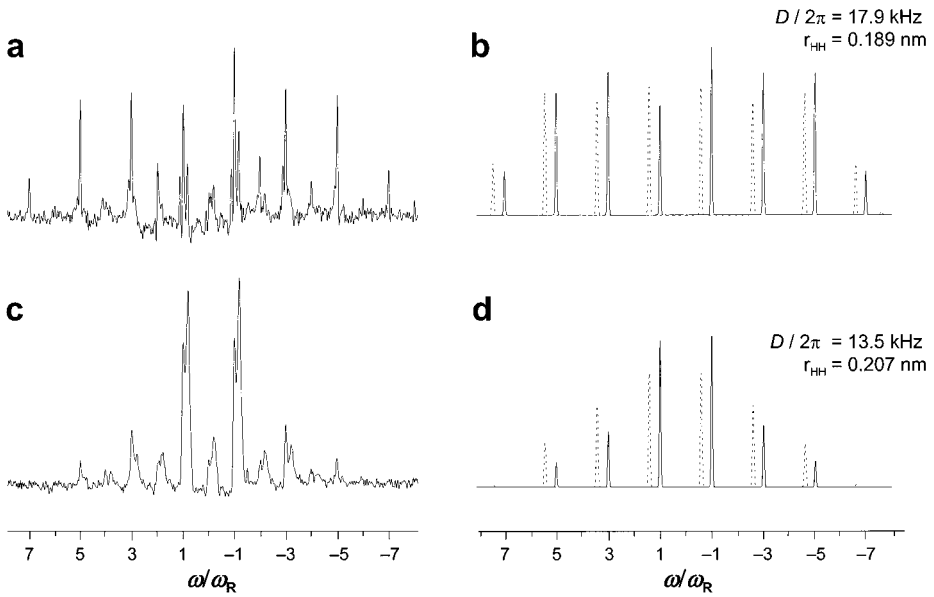

Figure 9. ^{1}H (700.1 MHz) DQ MAS NMR spinning-sideband patterns obtained for (a) the NH[1] hydrogen-bonded resonance of bilirubin, **1a**, and (c) the NH hydrogen-bonded resonances of the dimethyl ester of bilirubin, **1b**, obtained at a MAS frequency of 30 kHz using a BABA recoupling sequence of duration three rotor periods for the excitation and reconversion of DQCs. (b,d) The extracted experimental sideband patterns for the NH−NH DQCs are compared to spectra (dashed lines, displaced to the left of the experimental spectra) generated using the analytical time domain formula for an isolated spin pair,[8b,30a] obtained from a fitting of the extracted experimental integrated sideband intensities; the corresponding $D/2\pi$ values and internuclear distances are indicated.

bilirubin, an X-ray single-crystal structure exists such that an initial estimate of the geometrical arrangement was possible. However, simulated spectra demonstrated that a good reliability is also to be expected where no crystal structure can be obtained, e.g., materials in which there is local but not long-range order. Further improvements in spectral resolution are expected in the future, which will make solid-state NMR results even more reliable.

Our determination of the NH−NH distance within the bilirubin hydrogen-bonding arrangement to be 0.186 ± 0.002 nm proves an exceptionally close approach of two protons being noncovalently bonded to the same atom. This shows that the distances (namely 0.187 and 0.191 nm) obtained by Le Bas et al.[17] on the basis of a single-crystal X-ray analysis are reasonably accurate, despite the considerable difficulties associated with the localization of protons by X-ray diffraction. We also note that ab initio quantum chemical calculations, which will be presented elsewhere, preliminarily indicate a NH−NH distance of 0.187 nm.[44]

Solid-state NMR, at least at the present state of development, should not be considered as a replacement for the established scattering methods. Instead, the two methods should be thought of as being complementary, since they have much to offer each other. For example, in the case, as here, where it is possible to carry out a single-crystal X-ray analysis, ^{1}H DQ MAS and related heteronuclear techniques[27d,37,45] can provide additional

(44) Gauss, J., results to be published.

distance constraints such that important protons can be localized. In particular, the shifting of hydrogen-bonded resonances well away from the aliphatic peaks means that solid-state ^{1}H NMR methods are ideally suited to the investigation of what is often the most interesting part of the structure. Alternatively, the analysis of solid-state NMR spectra obtained for samples in which it was not possible to prepare a single crystal suitable for X-ray diffraction is greatly aided by the existence of X-ray single-crystal structures of related systems.[8a,b]

To conclude, we expect that ^{1}H solid-state NMR, and in particular DQ MAS spectroscopy, will develop into a method which is applied routinely to the investigation of a wide range of applications, from biology to materials science. In particular, solid-state NMR investigations of medium-sized proteins, fully labeled in ^{13}C and ^{15}N, are already being carried out;[3] a three-dimensional experiment linking a two-dimensional ^{1}H DQ MAS experiment with a ^{13}C or ^{15}N should be feasible for such systems and would be expected to give much useful information.

Experimental and Simulation Details

Bilirubin IXα (80% isomerically pure) and its dimethyl ester were purchased from Fluka and Porphorin Products, Inc, respectively, and used without further purification.

^{1}H MAS NMR experiments were performed on a Bruker DRX 700 narrow-bore spectrometer operating at a ^{1}H Larmor frequency of 700.1 MHz, using a double-resonance MAS probe supporting rotors of outer diameter 2.5 mm. A spinning frequency, ν_R, of 30 kHz was used. All experiments were performed using bearing gas at room temperature. At this very fast ν_R, the additional heating effect caused by air friction becomes significant. Using the ^{119}Sn resonance of $Sm_2Sn_2O_7$ as a chemical shift thermometer, the correction term relative to the bearing gas temperature has been calibrated in a separate study.[46] Unless otherwise stated, bearing gas at room temperature was used, corresponding to a true sample temperature of 321 K. The 90° pulse length was set equal to 2.0 μs, while a recycle delay of 3 s was used. For one-dimensional experiments, 8 (Figures 2a and S3) or 16 (Figure 2b) transients were averaged.

DQ MAS experiments were performed using the back-to-back (BABA) recoupling sequence[28] for the excitation ($p = 0 \rightarrow p = \pm 2$, where p is the coherence order) and reconversion ($p = \pm 2 \rightarrow p = 0$) of DQ coherence (DQC). The standard BABA sequence, of duration one rotor period, takes the form $P_x-\tau-P_{-x}-P_y-\tau-P_{-y}$, where P_ϕ denotes a radio frequency pulse with flip angle equal to 90° and phase ϕ, and τ equals $\tau_R/2$ minus the pulse durations. For longer excitation times, compensated variants based on the following two rotor-period sequence were used: $P_x-\tau-P_x-P_y-\tau-P_{-y}-P_x-\tau-P_x-P_{-y}-\tau-P_y$, whereby for excitation times longer than two rotor periods the sequence was repeated, changing all pulse phases by 180°.[47] Our DRX 700 spectrometer is not capable of fast phase switching, and thus it was necessary to include a 2 μs delay between the back-to-back pulses. After the reconversion sequence, a final 90° pulse creates transverse magnetization, with the duration of the $p = 0$ "z-filter" period set equal to one rotor period. The total phase cycle used[29] consisted of 16 steps with four steps to select $p = \pm 2$ after the excitation sequence and four steps to select $p = 0 \rightarrow p = -1$. Sign discrimination was restored in the F_1 dimension by the TPPI[48] or States-TPPI[49] method, which, in both cases, involves incrementing the phases of all excitation pulses by 45° after recording each t_1 point. For the States-TPPI approach, t_1 is incremented only after every second t_1 point; in this way, the DQ spectral width equals $1/\Delta t_1$, as opposed to $1/(2\Delta t_1)$ for the TPPI approach. In the rotor-synchronized experiments, the increment in t_1, Δt_1, has to be set equal to one rotor period, and thus the States-TPPI approach has the advantage of doubling the DQ spectral width.

In the rotor-synchronized experiments, the increment in t_1 was set equal to one rotor period, with, for each of 64 increments, 32 transients being averaged; the total experimental time was 102 min. In the contour plots, solid and dashed lines represent positive and negative contours, respectively, with the bottom contour corresponding to 6.0 and 12.0% of the maximum intensity in Figure 3a and 3b, respectively, and subsequent contours corresponding to a multiplicative increment of 1.2. To obtain the DQ MAS spinning-sideband patterns, 512 increments of 1.0 μs and 610 increments of 0.8 μs (corresponding to F_1 spectral widths of 500 and 625 kHz) were used in Figures 6b, 6d, and 9c and in Figure 6f, respectively, averaging over 32 (Figure 6b) or 48 transients (all other cases). The total experimental time was 14, 21, 24, and 21 h in Figures 6b, 6d, 6f, and 9c, respectively. The transmitter frequency was set to 7.0, 7.0, 6.0, 6.4, 6.8, and 7.0 ppm for the experiments in Figures 3a, 3b, 6b, 6d, 6f, and 9c, respectively. Displayed spinning-sideband patterns correspond to a sum over the SQ frequencies corresponding to the relevant SQ peak.

Numerical density matrix simulations were performed on a single-processor Unix workstation using a home-written C++ program. The Liouville−von Neumann equation was explicitly solved for stepwise increments (of the order of 1 μs) of the rotor phase. Powder averaging was performed over 8064 angles according to the REPULSION method.[50] A Gaussian line broadening of 2 kHz was applied. The fitting of the extracted experimental sideband intensities to spectra generated using the analytical spin-pair formula made use of the Numerical Recipes Levenberg−Marquardt least-squares fitting routine.[51]

Acknowledgment. S.P.B. and X.X.Z. thank the Alexander von Humboldt-Stiftung for the award of research fellowships. Helpful discussions with Dr. Ingo Schnell are acknowledged. We also thank Professor G. R. Brown for providing the bilirubin dimethyl ester sample.

Supporting Information Available: Three-spin density matrix simulated spectra which support the validity of the presented approach for the quantitative determination of proton−proton distances and geometry from DQ MAS NMR; the slight changes in the ^{1}H chemical shifts upon heating (PDF). This material is available free of charge via the Internet at http://pubs.acs.org.

JA004231H

(45) (a) Hohwy, M.; Jaroniec, C. P.; Reif, B.; Rienstra, C. M.; Griffin, R. G. *J. Am. Chem. Soc.* **2000**, *122*, 3218. (b) Van Rossum, B.-J.; de Groot, C. P.; Ladizhansky, V.; Vega, S.; de Groot, H. J. M. *J. Am. Chem. Soc.* **2000**, *122*, 3465. (c) Saalwächter, K.; Spiess, H. W. *J. Chem. Phys.* **2001**, *114*, 5707.

(46) Langer, B.; Schnell, I.; Spiess, H. W.; Grimmer, A.-R. *J. Magn. Reson.* **1999**, *138*, 182.

(47) Feike, M.; Demco, D. E.; Graf, R.; Gottwald, J.; Hafner, S.; Spiess, H. W. *J. Magn. Reson. A* **1996**, *122*, 214.

(48) Marion, D.; Wüthrich, K. *Biochem. Biophys. Res. Commun.* **1983**, *113*, 967.

(49) Marion, D.; Ikura, M.; Tschudin, R.; Bax, A. *J. Magn. Reson.* **1989**, *85*, 393.

(50) Bak, M.; Nielsen, N. *J. Magn. Reson.* **1996**, *125*, 132.

(51) Press, W. H.; Flannery, B. P.; Teukolsky, S. A.; Vetterling, W. T. *Numerical Recipes in C*; Cambridge University Press: Cambridge, 1991.